Chemical Physics Letters 597 (2014) 110–113

Contents lists available at ScienceDirect

Chemical Physics Letters

journal homepage: www.elsevier.com/locate/cplett

Photoelectron spectroscopic study of the diphenylphosphide anion and its oxide

Xinxing Zhang [a], Xin Tang [a], Dennis H. Mayo [b,c], Samantha DeCarlo [b], Bryan Eichhorn [b], Kit Bowen [a,*]

[a] Department of Chemistry, Johns Hopkins University, Baltimore, MD 21218, United States
[b] Department of Chemistry, University of Maryland at College Park, College Park, MD 20742, United States
[c] Research Department, Indian Head EOD Technology Division, Naval Surface Warfare Center, Indian Head, MD 20640, United States

ARTICLE INFO

Article history:
Received 22 January 2014
In final form 19 February 2014
Available online 28 February 2014

ABSTRACT

We have measured anion photoelectron spectra of the diphenylphosphide anion, PPh_2^-, and its oxide, $POPh_2^-$, the former being a ligand which is often utilized in inorganic chemistry. From these spectra, we have determined the vertical detachment energies of these anions and estimates of the electron affinities of their corresponding neutral molecules. We also conducted computations that provided structures of both the anions and their corresponding neutrals in both systems as well as electron affinities and vertical detachment energies in both systems. The calculated electron affinities and vertical detachment energies are in good agreement with the experimental values in both systems.

1. Introduction

Alkali metal diphenylphosphides are widely used as reagents in coordination chemistry [1–4]. Several of these compounds have been studied in solution by NMR [5] and in the solid state by X-ray crystallography [6]. From these investigations, it is known that the structure of the diphenylphosphide anion is strongly dependent on its interactions with its environment, e.g., with solvents [7], its coordination environment with transition metal ions or with alkali counter-cations [8,9]. Related species, such as the 'naked' phosphide anion in potassium crown ether salts are also known [10]. Thus far, however, there have been no studies of truly free organophosphide anions, i.e., in the gas phase. Among small phosphorus-containing anions, only PH^-, PH_2^-, PO^-, P_2^-, and PO_2^-, have been studied in the gas phase by anion photoelectron spectroscopy [11–13].

In the present work, we conducted a combined study using gas phase, anion photoelectron spectroscopy and density functional theory (DFT) to characterize the free diphenylphosphide anion (PPh_2^-). In addition, its oxide anion ($POPh_2^-$) was also studied in the same manner. The electron affinities (EA) and vertical detachment energies (VDE) of both species were measured and compared with our theoretical results. Calculated combustion enthalpies were also reported.

2. Methods

2.1. Experimental

Anion photoelectron spectroscopy is conducted by crossing a mass-selected beam of negative ions with a fixed-frequency photon beam and energy-analyzing the resultant photodetached electrons. It is governed by the energy-conserving relationship, $h\nu = EBE + EKE$, where $h\nu$ is the photon energy, EBE is the electron binding (photodetachment transition) energy, and EKE is the electron kinetic energy. Our anion photoelectron spectrometer, which has been described previously [14], consists of an infrared desorption/photoemission (IR/PE) anion source, a linear time-of-flight mass analyzer/selector, a pulsed Nd:YAG photodetachment laser (0.4–0.5 mJ per pulse into ~1 mm^2), and a magnetic bottle electron energy analyzer. Photoelectron spectra were calibrated against the well-known photoelectron spectrum of Cu^- [15].

The diphenylphosphide anion and its oxide were generated from a solid sample of the ligated aluminum cluster, $Li_2Al_3(PPh_2)_6$. Details of the sample's synthetic preparation are described elsewhere [16]. A unique anion source was employed that combines pulsed infrared desorption to bring molecules into the gas phase, pulsed photoemission to provide low-energy electrons for attachment, and a pulsed helium jet expansion to cool and transport of the resultant anions. This infrared desorption/photoemission (IR/PE) source has been previously described [17]. Briefly, a short IR pulse (1064 nm) from a Nd:YAG laser strikes a translating graphite bar thinly coated with sample. An almost simultaneous pulse of 532-nm light from a second Nd:YAG laser strikes a

* Corresponding author. Fax: +1 410 516 8420.
E-mail address: kbowen@jhu.edu (K. Bowen).

http://dx.doi.org/10.1016/j.cplett.2014.02.041
0009-2614/

photoemitter (Hf wire) creating a shower of low-energy electrons that attach to the evaporated neutral species. A plume of ultrahigh purity (UHP) helium gas expanded from a pulsed valve located upstream then cools the nascent plasma mixture and guides it toward the mass spectrometer, where it is analyzed. Due to the sample's air sensitivity, the crystalline $Li_2Al_3(PPh_2)_6$ sample was burnished onto the graphite bar and sealed in an air tight container inside a glove box, which was maintained with an oxygen-free nitrogen atmosphere, until it placed in the pre-purged source vacuum chamber.

2.2. Computational

DFT calculations were conducted by applying Becke's three parameter hybrid functional (B3LYP) [18–20] using the GAMESS software package [21,22] to determine the EA values of PPh_2 and $POPh_2$, and the VDE values of PPh_2^- and $POPh_2^-$. The B3LYP method has been found to be satisfactory for predicting excess electron binding energies for many molecular valence anions [23]. All geometries, including those of the anions and their corresponding neutral molecules, were fully optimized without any geometrical constraints while using the 6-31G(d,p) basis set. The electronic energies were then improved by single-point calculations with a larger basis set, i.e., aug-cc-pVTZ [24,25], at optimized geometries.

3. Results and discussion

The anion photoelectron spectra of PPh_2^- and $POPh_2^-$, both measured with 355 nm (3.49 eV) photons, are shown in Figure 1. The spectrum of PPh_2^- shows a relatively narrow peak with the hint of a weak vibrational progression, while that of $POPh_2^-$ shows a broad band. The adiabatic electron affinity, EA, is the energy difference between the lowest energy vibronic state of the anion and the lowest energy vibronic state of its neutral counterpart. We have estimated the EA values of PPh_2 and $POPh_2$ by extrapolating the low EBE side of their respective spectral bands to zero, with the extrapolated EBE values being taken as their electron affinities. Thus, we have determined the electron affinities of PPh_2 and $POPh_2$ to be 1.5 ± 0.1 eV and 2.2 ± 0.1 eV, respectively. Our calculated values are 1.53 eV and 2.00 eV, in good agreement with our experimental values. The EBE value at the intensity maximum of the lowest EBE band in a given photoelectron spectrum is the vertical detachment energy, VDE, of that anion, i.e., the transition energy at which the Franck Condon overlap between the wave functions of the anion and its neutral counterpart is maximal. We have determined the VDE values for PPh_2^- and $POPh_2^-$ to be 1.64 eV and 2.70 eV, respectively. Our calculated values of VDEs are 1.58 eV and 2.58 eV, also in good agreement with our experimentally-determined values. All the values, from both experiment and theory, are tabulated in Table 1.

Table 1
Experimental and theoretical electron affinities (EA) of PPh_2 and $POPh_2$, and vertical detachment energies (VDE) of PPh_2^- and $POPh_2^-$. All the numbers are in units of eV.

Species	EA		VDE	
	Theo.	Expt.	Theo.	Expt.
PPh_2/PPh_2^-	1.53	1.5 ± 0.1	1.58	1.64
$POPh_2/POPh_2^-$	2.00	2.2 ± 0.1	2.58	2.70

Figure 2 exhibits the optimized structures of PPh_2 and PPh_2^-. The small structural difference between the anion and the neutral implies that there should be a substantial Franck–Condon overlap between the 0' (anion) to 0' (neutral) transition, which is consistent with the sharp peak in the spectrum. Weaker 0' to 1' and 2' transitions, however, reflect the fact that the anion and neutral structures are not quite identical. Figure 3 shows the highest occupied molecular orbital (HOMO) of PPh_2^-. One observes that the excess electron is delocalized across the entire ion, with electronic communication between the two slightly off-plane benzene rings. The EA of PPh_2 measured here is higher than that of PH_2 (1.27 eV) [11], which is probably due to the stabilization by the two benzene rings. The optimized structures of $POPh_2$ and $POPh_2^-$ (Figure 4) show that the two benzene rings in the neutral are much closer to lying in the same plane than those in the anion. This structural difference resulted in the observed broad spectral band.

Small, low oxidation state aluminum-containing clusters are of great interest as energetic materials [26]. The compound used in this work, $Li_2Al_3(PPh_2)_6$, is an example of such a species, where the PPh_2^- ligands have helped to stabilize the aluminum trimer core. In the course of combustion of such compounds, there is an interest

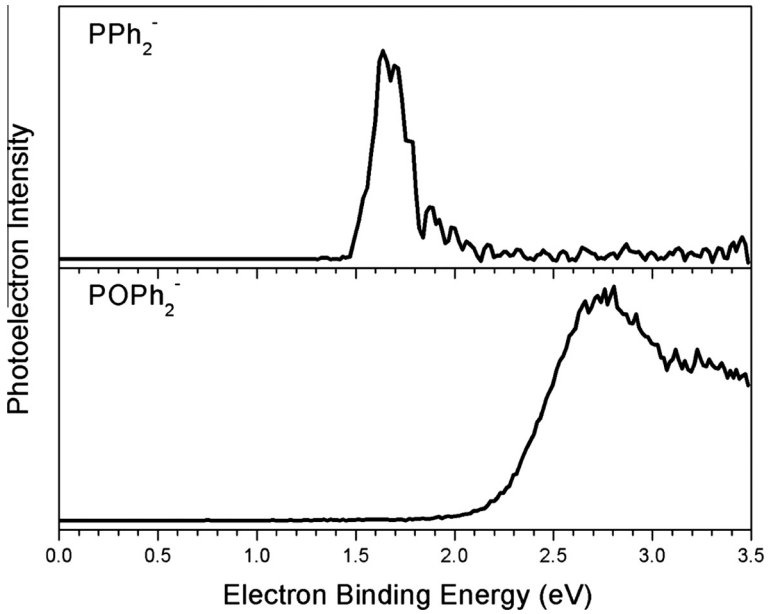

Figure 1. Anion photoelectron spectra of the diphenylphosphide anion (PPh_2^-) and its oxide ($POPh_2^-$), both recorded with 355 nm (3.49 eV) photons.

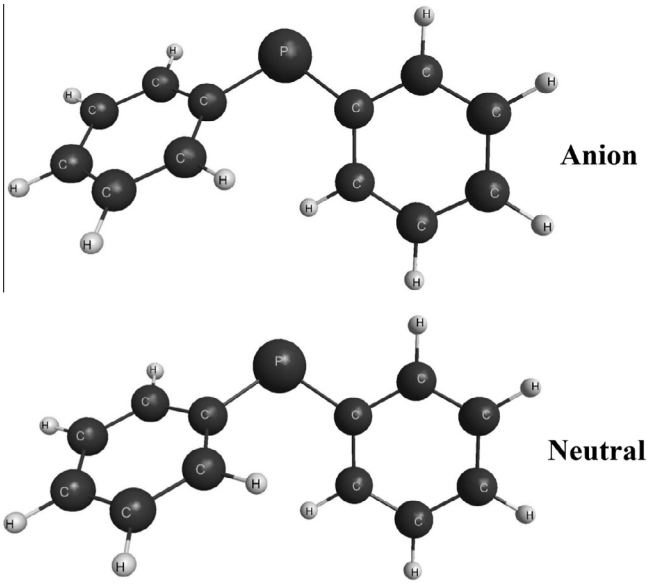

Figure 2. The optimized structures of PPh_2 and PPh_2^-, calculated using the B3LYP/6-31G (d, p) method.

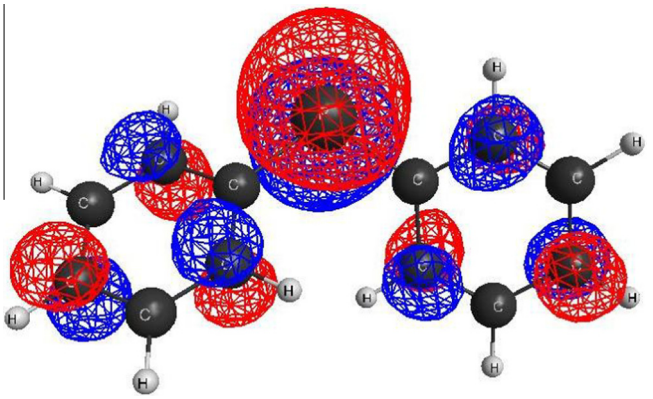

Figure 3. The highest occupied molecular orbital (HOMO) of PPh_2^-, calculated at the B3LYP/ aug-cc-pVTZ level of theory.

in knowing the heats of combustion of the ligands as well as of the aluminum core. Our DFT calculations found

$$PPh_2 + 1/2O_2 \rightarrow POPh_2,$$

and

$$PPh_2^- + 1/2O_2 \rightarrow POPh_2^-$$

to have combustion enthalpies (ΔH_c) of −50 kcal/mol and −61 kcal/mol, respectively. Note that $EA(POPh_2) - EA(PPh_2) = \Delta H_c(PPh_2) - \Delta H_c(PPh_2^-)$. Our calculated combustion enthalpies are consistent with our calculated EA values. Compared to the combustion of bulk aluminum ($\Delta H_c = -200$ kcal/mol), the energy released from the oxidation of these ligands is much smaller.

Considering the fact that the activation energy for the oxidation of aluminum nanoparticles was found to be much smaller than that of bulk aluminum samples [27], and the ignition temperature of aluminum nanoparticles is significantly lower than that of micron-sized aluminum [28], the small aluminum core in $Li_2Al_3(PPh_2)_6$ should be far more readily oxidized than bulk aluminum.

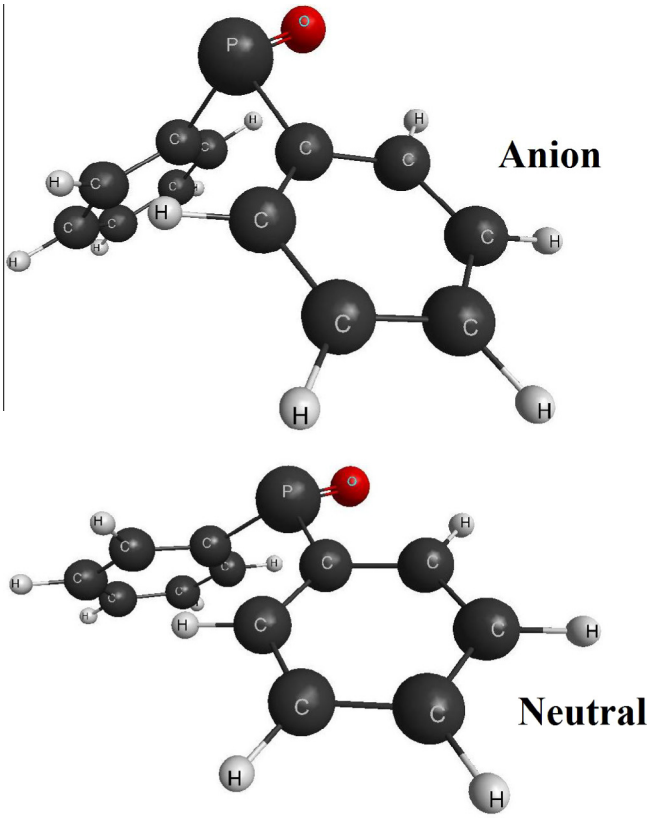

Figure 4. The optimized structures of $POPh_2$ and $POPh_2^-$, calculated using the B3LYP/6-31G (d, p) method.

Acknowledgements

This material is based upon work supported by the Defense Threat Reduction Agency (DTRA) and by the Air Force Office of Scientific Research (AFOSR) under Grant numbers, HDTRA-1-12-1-007 (BWE, DHM, & KHB) and FA95501110068 (KHB), respectively.

References

[1] H.C. Aspinall, S.R. Moore, A.K. Smith, J. Chem. Soc. Dalton Trans. 1992 (1992) 153.
[2] C.M. Alvarez, M.E. Garcia, M.A. Ruiz, Organometallics 23 (2004) 4750.
[3] S.M. Cendrowski-Guillaume, M. Ephritikhine, J. Organomet. Chem. 577 (1999) 161.
[4] D.O. Downing, P. Zavalij, B.W. Eichhorn, Inorg. Chim. Acta 375 (2011) 329.
[5] I.J. Colquhoun, H.C.E. McFarlane, W. McFarlane, J. Chem. Soc., Chem. Commun. 1982 (1982) 220.
[6] H. Hope, M.M. Olmstead, P.P. Power, X. Xu, J. Am. Chem. Soc. 106 (1984) 819.
[7] V.A. Zschunke, E. Bauer, H. Schmidt, K. Issleib, Z. Anorg. Allg. Chem. 495 (1982) 115.
[8] D.H. Mayo, Y. Peng, S. DeCarlo, X. Li, J. Lightstone, P. Zavalij, K. Bowen, H. Schnöckel, B. Eichhorn, Z. Anorg. Allg. Chem. 639 (2013) 2558.
[9] M. Pfeiffer, T. Stey, H. Jehle, B. Klüpfel, W. Malisch, V. Chandrasekhar, D. Stalke, Chem. Commun. 2001 (2001) 337.
[10] V.L. Rudzevich, H. Gornitzka, K. Miqueu, J.-M. Sotiropoulos, G. Pfister-Guillouzo, V.D. Romanenko, G. Bertrand, Angew. Chem., Int. Ed. 41 (2002) 1193.
[11] P.F. Zittel, W.C. Lineberger, J. Chem. Phys. 65 (1976) 1236.
[12] J.T. Snodgrass, J.V. Coe, C.B. Freidhoff, K.M. McHugh, K.H. Bowen, Chem. Phys. Lett. 122 (1985) 352.
[13] C. Xu, E. de Beer, D.M. Neumark, J. Chem. Phys. 104 (1996) 2749.
[14] M. Gerhards, O.C. Thomas, J.M. Nilles, W.J. Zheng, K.H. Bowen, J. Chem. Phys. 116 (2002) 10247.
[15] J. Ho, K.M. Ervin, W.C. Lineberger, J. Chem. Phys. 93 (1990) 6987.
[16] Mayo, D. H. Synthesis and Characterization of Low-Valent Aluminum and Gallium Compounds From Metastable Aluminum (I) and Gallium (I) Precursors. Ph.D Dissertation, University of Maryland, College Park, MD, 2011.
[17] S.T. Stokes, X. Li, A. Grubisic, *J. Chem. Phys.* 127 (2007) 084321.
[18] A.D. Becke, Phys. Rev. A 38 (1988) 3098.

[19] A.D. Becke, *J. Chem. Phys.* 98 (1993) 5648.
[20] C. Lee, W. Yang, R.G. Parr, Phys. Rev. B 37 (1988) 785.
[21] M.W. Schmidt, K.K. Baldridge, J.A. Boatz, S.T. Elbert, M.S. Gordon, J.H. Jensen, S. Koseki, N. Matsunaga, K.A. Nguyen, S.J. Su, T.L. Windus, M. Dupuis, J.A.J. Montgomery, *J. Comput. Chem.* 14 (1993) 1347.
[22] M. S. Gordon, M. W. Schmidt, C. E. Dykstra, G. Frenking, K. S. Kim, and G. E. Scuseria, Theory and Applications of Computational Chemistry: The First Forty Years, (Elsevier, 2005), pp. 1167.
[23] J.C. Rienstra-Kiracofe, G.S. Tschumper, H.F. Schaefer, S. Nandi, G.B. Ellison, *Chem. Rev.* 102 (2002) 231.
[24] D.E. Woon, T.H. Dunning Jr., *J. Chem. Phys.* 90 (1989) 1007.
[25] D.E. Woon, T.H. Dunning Jr., *J. Chem. Phys.* 98 (1993) 1358.
[26] K.S. Williams, J.P. Hooper, J. Phys. Chem. A 115 (2011) 14100.
[27] C.E. Aumann, G.L. Skofronick, J.A. Martin, J. Vac. Sci. Technol., B 13 (1995) 1178.
[28] T. Bazyn, H. Krier, N. Glumac, Combust. Flame 145 (2006) 703.